Electrons and phonons in quantum wells

© J. Požela¶, A. Namajūnas, K. Požela, V. Jucienė

Semiconductor Physics Institute,
2600 Vilnius, Lithuania

(Получена 1 марта 1999 г. Принята к печати 2 марта 1999 г.)

The modulation of electron and polar optical phonon states in an AlGaAs/GaAs/AlGaAs quantum well (QW) with an inserted thin AlAs barrier is considered. The OW width dependence of electron–phonon scattering rates are estimated. The great contribution to the change of electron subband population, photovoltaic effect and electron mobility in the QW gives the resonant intersubband scatteting of electrons by interface phonons. The decrease of electron mobility limited by polar optical phonon scattering with increasing carrier concentration in the QW is established. The conditions for the increase of mobility in the QW by inserting the AlAs barrier are found.

Introduction

The confinement of electrons and phonons in semiconductor quantum wells (QW's) improves their electrical and optical properties with respect to bulk materials. Semiconductor QW structures have received great attention, because of their potential for laser operating in the infrared region [1-3], nonlinear optical elements, infrared photoelectric detectors [4]. The enhancement of electron mobility in QW's has attracted increasing attention by many authors [5–14].

In the paper the role of modulation of electron and polar optical (PO) phonon states in AlGaAs/GaAs/AlGaAs QW's in the change of electron mobility, photoexcited electron subband population and photovoltaic effect is considered. The conditions for electron mobility enhancement and for inversion of photoexcited electron subband population are determined. The consideration is carried out for the case of AlGaAs/GaAs/AlGaAs structure with and without an inserted AlAs barrier (fig. 1).

The paper is organized as follows. In Sec. 1 the peculiarities of electron–phonon scattering rate in QW's are considered. The dependencies of photoexcited electron subband population and photovoltaic effect on intersubband scattering rates are determined in Secs. 2 and 3. The contrubution of intra- and intersubband electron–PO-phonon scattering to the electron mobility in the QW is calculated in Sec. 4.

1. Electron–PO-phonon scattering rate in a quantum well

According of the Fermi Golden Rule, the frequency of transitions of electros, confined in the QW, from the initial state $\mathbf{k}_i$, E_{si} to any final states $\mathbf{k}_f$, E_{sf} in all f electron subbands by emission (absorption) of all ν-modes of PO phonons can be written as

$$W^{\pm}(k_i, E_{si}) = \sum_{\nu} \sum_{f} \sum_{\mathbf{k}_f} \frac{4\pi m e^2}{\hbar^3} |G_{\nu}(z)|^2 \times F_{q\nu} \left(N_{q\nu} + \frac{1}{2} \pm \frac{1}{2} \right) \delta(k_f^2 - k_i^2 + \beta_{\pm}), \quad (1)$$

$$G_{\nu}(z) = \int_{L_e} \varphi_{e1}(z) \varphi_{e2}(z) \varphi_{q\nu}(z) dz, \quad (2)$$

where z is the quantization direction, L_e is the area where electron wave function $\varphi_{ei} \neq 0$, m, e, $\mathbf{k}_i$, E_{si}, φ_{ei} are the electron mass, charge, wave vector, subband energy, and normalized wave function, respectively, $\varphi_{q\nu}(z)$ is the z-component of ν-mode phonon potential function, $N_{q\nu}$ is the number of ν-mode phonons, and

$$\beta_{\pm} = \frac{2m}{\hbar^2}(E_{sf} - E_{si} \pm \hbar\omega_{\nu}). \quad (3)$$

The upper (plus) sign is for phonon emission and the lower (minus) one is for phonon absorption.

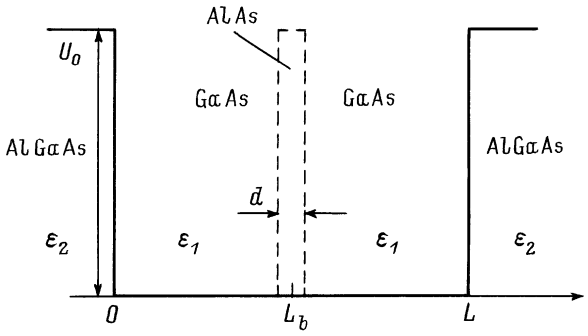

Figure 1. Schematic view of an $Al_{0.3}Ga_{0.7}As/GaAs/Al_{0.3}Ga_{0.7}As$ QW structure. L is the QW width, L_b is the position of a thin AlAs barrier with the thickness d. $U_0 = 0.3$ eV is the heterojunction potential.

¶ E-mail: pozela@uj.pfi.lt

In the dielectric continuum approach the square of phonon normalization coefficient can by written as [11]

$$F_{q\nu} = \frac{\hbar}{S}\left[\left(\frac{d\varepsilon_1}{d\omega}\right)_\nu \int_1 f_\nu dz + \left(\frac{d\varepsilon_2}{d\omega}\right)_\nu \int_2 f_\nu dz\right]^{-1}, \quad (4)$$

where S is the in-plane of normalization area, ε_1 and ε_2 are the dielectric functions, and

$$f_\nu = q_{0\nu}^2 |\varphi_{q\nu}|^2 + \left|\frac{d\varphi_{q\nu}}{dz}\right|^2,$$

where $q_{0\nu}$ is the wave vector of emitted (absorbed) ν-mode phonon in the plane of QW:

$$q_{0\nu}^2 = k_i^2 + k_f^2 - 2k_i k_f \cos\theta, \quad k_f^2 = k_i^2 + \beta_\pm, \quad (5)$$

where θ is the angle between the initial wave vector $\mathbf{k}_i$ and the final one $\mathbf{k}_f$. The subscripts 1 and 2 correspond to the QW and barrier regions, respectively.

The electron wave functions are obtained by solving the Schrödinger equation for the QW under consideration. The phonon potentials are obtained by solving the Laplace's equation by using dielectric continuum approach. The phonon potentials in the AlGaAs/GaAs/AlGaAs QW with a thin AlAs barrier can be divided into three separate branches: interface phonons localized at the AlAs barrier with the potential φ_q^B, interface localized at the AlGaAs/GaAs heterojunction with the potential φ_q^{HJ}, and confined phonons with the potential φ_q^C.

Using Eq. (1) and the calculated expressions for the electron wave function and phonon potentials, the electron–phonon scattering rates by various phonon branches can be obtained. For the confined electron scattering rate by confined phonons

$$W_{if}^{C\pm} = F_C^\pm \sum_{n=1}^{\infty} |G_C(z)|^2 \frac{2}{L} \int_0^{2\pi} \frac{d\theta}{(q_\nu^2 + q_z^2)}, \quad (6)$$

with

$$F_C^\pm = \frac{me^2}{2\pi\hbar^3}\left(N_{qC} + \frac{1}{2} \pm \frac{1}{2}\right)\frac{\hbar\omega_0}{2}\left(\frac{1}{\varepsilon_{1\infty}} - \frac{1}{\varepsilon_{1s}}\right), \quad (7)$$

$$G_C(z) = \int_{L_e} \varphi_{ei}\varphi_{ef}\sin(q_z z)dz, \quad q_z = n\frac{\pi}{L}, \quad (8)$$

where $\hbar\omega_0$ is the energy of a bulk longitudinal phonon, $\varepsilon_{1\infty}$ and ε_{1s} are the high-frequency and static dielectric constants, respectively, and L is the QW width.

For the confined electron scattering by the heterojunction ν-mode interface phonon at $qL > 2$

$$W_{if\nu}^{HJ\pm} = F_{IF\nu}^\pm \int_0^{2\pi} |G_{HJ\nu}(z)|^2 \frac{d\theta}{2q_{0\nu}}, \quad (9)$$

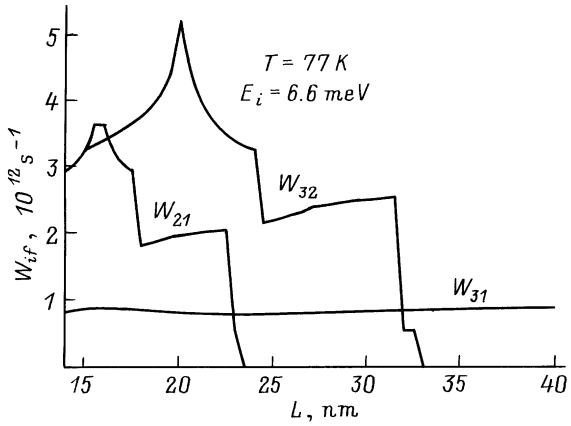

Figure 2. The QW width dependence of the intersubband scattering rates W_{if} between i- and f-subbands for electrons with kinetic energy $E_i = 6.6$ meV.

where

$$F_{IF\nu}^\pm = \frac{me^2}{2\pi\hbar^3}\left(N_{q\nu} + \frac{1}{2} \pm \frac{1}{2}\right)\hbar\left[\left.\frac{d\varepsilon_1}{d\omega}\right|_\nu + \left.\frac{d\varepsilon_2}{d\omega}\right|_\nu\right]^{-1}, \quad (10)$$

$$G_{HJ\nu}(z) = \int_{L_e} \varphi_{ei}\varphi_{ef}\varphi_{q\nu}^{HJ}dz. \quad (11)$$

For the confined electron scattering by the barrier ν-mode interface phonons at $qL > 2$, $qd \ll 1$

$$W_{if\nu}^B = F_{if\nu}^\pm \int_0^{2\pi} |G_{B\nu}(z)|^2 \frac{d\theta}{2q_{0\nu}}, \quad (12)$$

where

$$G_{B\nu}(z) = \int_{L_e} \varphi_{ei}\varphi_{ef}\varphi_{q\nu}^B dz. \quad (13)$$

The frequency of the confined phonons is equal to the longitudinal PO phonon frequency in a bulk GaAs $\hbar\omega_0 = 36.2$ meV. The frequencies of the heterojunction interface phonons at $qL > 2$ are $\hbar\omega_\nu = 33.1$, 35.4 and 45.9 meV. The frequencies of the interface phonons at the AlAs barrier at $qd \ll 1$, (where d is the barrier thickness) are $\hbar\omega_\nu = 36.2$ and 50.1 meV.

The electron–phonon scattering rates depend significantly on a QW width. The main peculiarity of this dependence is a very sharp change of the intersubband scattering rate at the QW width at which the electron intersubband energy becomes equal to the phonon energy. In this case the emitted (absorbed) phonon wave vector $\mathbf{q}_0 \to 0$ (see Eq. (5)), and the scattering rates proportional to q_0^{-1} are sharply increased. Fig. 2 illustrate the QW width dependence of the intersubband scattering rate (which includes scattering by all phonon modes).

2. Photoexcited electron subband population in a quantum well

Let us calculate the intersubband distribution of electrons photoexcited from the valence band to the third subband of the conduction band. The balance equations for nonequilibrium photoelectron subband population n_i in three subband levels are

$$\alpha_3 I_g - W_{31}n_3 - W_{32}n_3 + W_{13}n_1 + W_{23}n_2 = W_{03}n_3 \equiv I_3,$$

$$\alpha_2 I_g + W_{32}n_3 - W_{21}n_2 - W_{23}n_2 + W_{12}n_1 = W_{02}n_2 \equiv I_2,$$

$$\alpha_1 I_g + W_{31}n_3 + W_{21}n_2 - W_{13}n_1 - W_{12}n_1 = W_{01}n_1 \equiv I_1, \quad (14)$$

where $a_i I_g$ is the flow of photoexcited electrons downs to i-subband bottom, which is proportional to the intensity I_g of photolumicescence (PL) excitation source and to the probability $\alpha_i \sim \langle [1 - f(E)] \rangle$ that the subband bottom electron state is not occupied,

$$W_{if} = \langle W_{if}(E)[1 - f(E \pm h\omega)] \rangle \quad (15)$$

is the intersubband transition rate, W_{0i} is the exciton formation rate (we assume that the radiative transitions through the electron-hole exciton states are dominant), and I_i are the PL peak intensities which are proportional to i-subband photoexcited electron population. The brackets $\langle\ \rangle$ means the average value:

$$\langle A \rangle = \int A f(E) dE \Big/ \int f(E) dE, \quad (16)$$

where $f(E)$ is the Fermi-Dirac distribution function. We normalize the PL peak intensities: $I_1 + I_2 + I_3 = 1$, and suppose $I_g = 1$ and $\alpha_1 + \alpha_2 + \alpha_3 = 1$.

Fig. 3 shows the calculated QW width dependence of PL peak intensity in the $Al_{0.3}Ga_{0.7}As/GaAs/Al_{0.3}Ga_{0.7}As$ structure. One can see that at $17 < L < 26$ nm the inversion of photoexcited electron population on the second and on the first subbands takes place. At these QW widths the

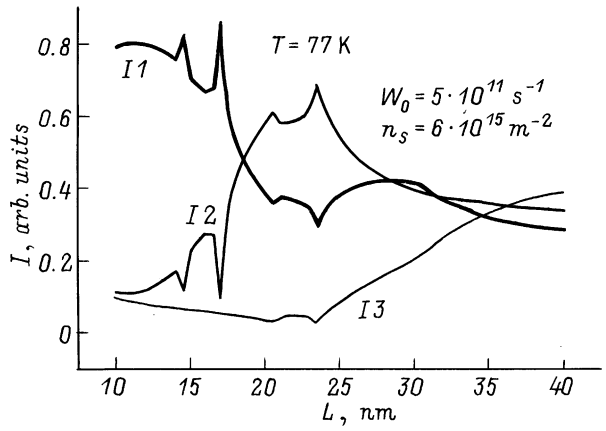

Figure 3. The well width dependence of PL peaks I_i corresponding to subbands i in the $Al_{0.3}Ga_{0.7}As/GaAs/Al_{0.3}Ga_{0.7}As$ quantum well.

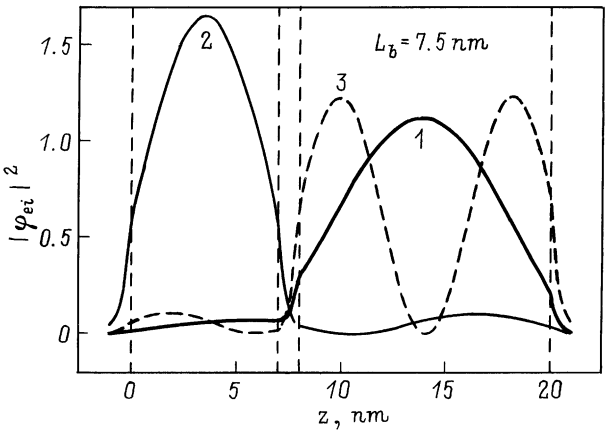

Figure 4. The dependence of electron wave function square $|\varphi_{ei}|^2$ on a coordinate z across the QW in the three lower subbands (1, 2, 3) in GaAs QW of width $L = 20$ nm with 1 nm AlAs barrier inserted at $L_b = 7.5$ nm.

subband energy separation between the third and the second subbands is larger than the confined and interface phonon energies, and between the second and the first subbands is less than these energies. As a result, $W_{32} \gg W_{21}$. It is the main criteria for achieving the population inversion in the QW. The inversion in PL peak intensities ($I_2 > I_1$) has been observed experimentally [15].

3. Electron in asymmetric coupled quantum wells. Photovoltaic effect

The insertion of thin AlAs barrier into the GaAs quantum well (QW) deforms the electron wave function φ_e. Fig. 4 shows the variation of $|\varphi_e|^2$ across the QW of width $L = 20$ nm for the three lower electron subbands when the barrier is inserted. One can see that the distribution of the electron charge across the QW in the subbands is nonsymmetric. Due to the deformation of the electron wave function the voltage across the QW arises.

The photovoltaic potential arises across the asymmetric coupled QW when the electrons are photoexcited from the first subband to the second one due to different electron charge deformation in these subbands

$$V_{p\nu} = \frac{e}{\varepsilon_1} \Delta n \int_{L_1}^{L_2} \left[\int_{L_1}^{z} (|\varphi_{e1}(z')|^2 - |\varphi_{e2}(z')|^2) dz' \right] dz. \quad (17)$$

$L_2 - L_1$ is the area, where $|\varphi_{ei}|^2 \neq 0$.

The calculated photovoltaic voltage for the case when the AlAs barrier is inserted in the QW at $L_b = 7.5$ nm, and when electrons with the concentration $\Delta n = 8 \times 10^{14}\ m^{-2}$ are photoexcited from the first subband to the second one, is equal to 2.2 mV. The photovotaic effect in asymmetric coupled QW's can be used for the detection of infrared radiation. The photovoltaic response to the radiation which

excites the electrons from the first QW subband to the second one is equal

$$\frac{V_{p\nu}}{P} = \frac{e}{\varepsilon_1}\frac{W_{32}}{W_{21}(W_{31}+W_{32})h\nu_{13}} \times \int_{L_1}^{L_2}\left[\int_{L_1}^{z}(|\varphi_{e1}(z')|^2 - |\varphi_{e2}(z')|^2)dz'\right]dz, \quad (18)$$

where P and $h\nu_{13}$ are the power and energy of the optical excitation signal. This signal is proportional to the W_{21}^{-1} which can be done large when $E_{s2} - E_{s1} < \hbar\omega_0$.

4. Electron mobility in the quantum well

Let us estimate the contribution of PO phonon confinement in the QW to the electron mobility in the $Al_{0.3}Ga_{0.7}As/GaAs/Al_{0.3}Ga_{0.7}As$ QW with and without the inserted thin AlAs barrier. The electron mobility limited by PO phonon scattering we shall estimate in the relaxation time approximation. The relaxation time τ_r of the perturbed electron state $\mathbf{k}_i$ to the equilibrium state $\mathbf{k}_f$ [16]

$$\frac{1}{\tau_r(\mathbf{k}_i)} = \sum_{\mathbf{k}_f}\{W_{if}[1-f(\mathbf{k}_f)] + W_{fi}f(\mathbf{k}_f)\} = \sum_{\mathbf{k}_f} W_{if}\frac{1-f(\mathbf{k}_f)}{1-f(\mathbf{k}_i)} \quad (19)$$

is involved as momentum relaxation time. Here $f(\mathbf{k})$ is the Fermi–Dirac distribution function and W_{if} is the probability of electron transition from the state i to the state f. In the parabolic subbands we have for electrons with energy E in the subband i

$$\frac{1}{\tau_{ri}(E)} = \sum_{\nu}\sum_{f} W_{if\nu}^{\pm}\frac{1-f(E\mp\hbar\omega_\nu)}{1-f(E)}, \quad (20)$$

where ν and f are the numbers of phonon mode and electron subband, respectively. The upper (plus-minus) sign is for phonon emission and lower one is for phonon absorption. The $W_{if\nu}^{\pm}$ is determined for each phonon mode by Eq. (1). The mobility of subband i electrons is

$$\mu_i = \frac{e}{m}\left\langle\frac{1}{\tau_{ri}(E)}\right\rangle^{-1}. \quad (21)$$

The average mobility in the QW

$$\mu = \sum_i \mu_i n_i/n_0, \quad (22)$$

where

$$n_i = D\int_{E_i}^{\infty} f(E)dE \quad (23)$$

is the concentration of electrons in the subband i, $D = m/\pi\hbar^2$ and $n_0 = \sum_i n_i$.

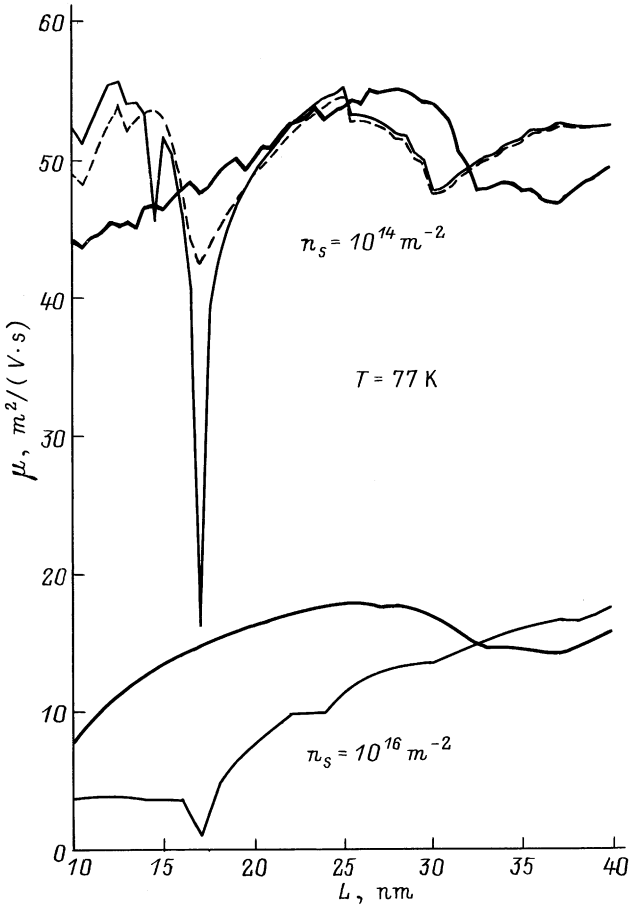

Figure 5. The electron mobility as a function of QW width L at $T = 77\,\mathrm{K}$ for $n_S = 10^{14}\,\mathrm{m}^{-2}$ (upper curves) and for $n_S = 10^{16}\,\mathrm{m}^{-2}$ (lower curves). The thick and thin solid lines correspond to electron–phonon scattering in the QW with and without inserted barrier, respectively. The dashed lines correspond to the electron scattering by confined phonons only in the QW without the barrier.

It is known that the relaxation time approximation gives only crude estimation of the mobility limited by PO phonon scattering, but it is expected this approximation to be sufficient for the purpose in which we are interested: only in relative difference between the mobilities in QW's with different widths and in the relative contribution to electron mobility of various electron scattering mechanisms by various phonon modes.

Note that values of mobility calculated in the used relaxation time approximation in bulk GaAs ($\mu = 50\,\mathrm{m}^2/(\mathrm{V}\cdot\mathrm{s})$ at $T = 77\,\mathrm{K}$ and $\mu = 0.65\,\mathrm{m}^2/(\mathrm{V}\cdot\mathrm{s})$ at $T = 293\,\mathrm{K}$) are near to the experimentally observed values.

Fig. 5 shows the calculated well width dependencies of electron mobility in the AlGaAs/GaAs/AlGaAs QW. The dependencies are characterized by the superposition of the two type minima: the smooth (sawtooth-like) minima and the sharp ones. The sharp minina correspond to the resonant increase of electron scattering rates by the interface phonons when the subband energy separation

becomes equal to the heterojunction interface phonon energies. This situation takes place at $L = 14$ and 16–17 nm. The neglect of scattering by the interface phonons taking into account only confined phonon scattering shows that the smooth (sawtooth-like) dependence are determined by two competing effects. The first effect is the reduction in the strength of the electron-confined phonon interaction, leading to the mobility enhancement proportionally to the increase of the QW width L (see Eq. (6)). The second one is the decrease of the electron mobility at QW widths when the intersubband scattering by absorption of the confined phonon from the lower subband to the second one (at $L = 16$ nm) and to the third subband (at $L = 30$ nm) becomes energetically possible ($\Delta E_{if} \leqslant \hbar\omega_0$).

At low electron concentration ($n_S = 10^{14}\,\mathrm{m}^{-2}$) the mobility in the QW of width $L = 10-15$ nm, $L = 20-30$ nm, and $L > 35$ nm is slightly large than in a bulk material. The increase of electron concentration ($n_S = 10^{16}\,\mathrm{m}^{-2}$) in the QW decreases drastically the electron mobility limited by PO phonon scattering (see fig. 5). The rise of the electron energy in the lower subband due to the electron degeneration is responsible for the strong enhancement of the intersubband scattering rate by the confined phonons, and, consequently, for the decrease of the electron mobility.

One can see that the confinement of electrons and phonons in the AlGaAs/GaAs/AlGaAs HEMT channels does not enhance the electron mobility limited by PO phonon scattering. Moreover, the increase of the carrier concentration in the channel decreases significantly the electron mobility. Note, that mobility measured experimentally in the AlGaAs/GaAs/AlGaAs QW's is lower than in a bulk GaAs. In the QW of width $L = 15-20$ nm at $T = 80$ K $\mu = 4\,\mathrm{m}^2/(\mathrm{V}\cdot\mathrm{s})$ at $n_S = 10^{16}\,\mathrm{m}^{-2}$ [7], and $\mu = 6\,\mathrm{m}^2/(\mathrm{V}\cdot\mathrm{s})$ at $n_S = 10^{15}\,\mathrm{m}^{-2}$ [6]. These experimental data are near to the calculated mobilities (see fig. 5). This mobility decrease can be compensated by inserting thin AlAs barrier into the QW which is transparent to electrons but reflects PO phonons. We have named this barrier phonon wall [17].

The insertion of the barrier into the center of the QW changes the electron subband energy spectra. The subband energies are grouped into pairs with increasing the separation energy between the pairs. This separation energy becomes comparable with the phonon energy only at $L \geqslant 30$ nm. As a result, the sharp resonant peaks of the mobility disappear and the positions of the wide mobility minimum shift to large QW widths. This is shown in Fig. 5. The especially large increase of the mobility is observed in the case of high electron sheet concentration ($n_S = 10^{16}\,\mathrm{m}^{-2}$). In the case of low electron sheet concentration ($n_S = 10^{14}\,\mathrm{m}^{-2}$) the insertion of the barrier increases the electron mobility in the QW in the interval of widths $16 < L < 31$ nm. Note that in this interval the increase of electron mobility was observed experimentally [6].

Conclusions

It is shown that the polar optical phonon confinement in QW's effects strongly the electron–phonon scattering strength. The resonant increase of the intersubband electron–phonon scattering rate takes place when the energy of the interface phonons becomes equal to the subband energy separation in the QW. At QW widths which correspond to the resonance conditions the electron subband population and mobility change sharply.

The inversion of photoexcited electron subband population and electron mobility enhancement in the QW can be achieved for appropriate values of parameters for which intersubband scattering is reduced.

The increase of electron–phonon scattering rate when the enhancement of electron concentration in the QW takes place is responsible for the great decrease of electron mobility in the lower subbands. This decrease can be partly compensated by inserting a thin AlAs barrier into the GaAs QW.

The insertion of the thin barrier into the QW deforms the electron wave function differently in various subbands, and the photovoltaic effect occurs when the intersubband electron photoexcitation takes place.

References

[1] F.H. Julien, A. Sa'ar, J. Wang, J.-P. Leburton. Electron. Lett., **31**, 838 (1995).
[2] P. Boucaud, F.H. Julien, D.D. Yang, J.M. Lourtioz, E. Rosencher, P. Bois, J. Nagle. Appl. Phys. Lett., **57**, 3 (1990).
[3] J. Faist, F. Capasso, D. Sivco, C. Sirtori, A.L. Hutchinson, S.N.G. Chu, A.Y. Cho. Science, **264**, 553 (1994).
[4] B.F. Levine. J. Appl. Phys., **74**, R1 (1993).
[5] T. Tsuchiya, T. Ando. Phys. Rev. B, **48**, 4599 (1993).
[6] X.T. Zhu, H. Goronkin, G.N. Maracas, R. Droopad, M.A. Stroscio. Appl. Phys. Lett., **60**, 2141 (1992).
[7] I. Inoue, T. Matsuno. Phys. Rev. B, **47**, 3771 (1993).
[8] K. Yokoyama, K. Hess. Phys. Rev. B, **33**, 5595 (1986).
[9] N. Mori, T. Ando. Phys. Rev. B, **40**, 6175 (1989).
[10] H. Rücker, E. Molinary, P. Lugli. Phys. Rev. B, **45**, 6747 (1992).
[11] I. Lee, S.M. Goodnick, M. Gulia, E. Molinaty, P. Lugli. Phys. Rev. B, **51**, 7046 (1995).
[12] B.K. Ridley. Phys. Rev. B, **39**, 5282 (1989).
[13] J. Požela, V. Juncienė, K. Požela. Semicond. Sci. Technol., **10**, 1555 (1995).
[14] X. Zianni, C.D. Simserides, G.P. Triberis. Phys. Rev. B, **55**, 16 324 (1997).
[15] J. Požela, V. Juciene, A. Namajūnas, K. Požela, V.G. Mokerov, Yu.V. Fedorov, V.E. Kaminskii, A.V. Hook. J. Appl. Phys., **82**, 5564 (1997).
[16] В.Ф. Гантмахер, И.Б. Левинсон. *Рассеяние носителей тока в металлах и полупроводниках* (М., Наука, 1984) с. 50.
[17] J. Požela, V. Juciene, A. Namajūnas, K. Požela. J. Appl. Phys., **81**, 1775 (1997).

Редактор Т.А. Полянская